FGF21 Analogs of Sustained Action Enabled by Orthogonal Biosynthesis Demonstrate Enhanced Antidiabetic Pharmacology in Rodents

James Mu,[1] Jason Pinkstaff,[2] Zhihua Li,[1] Lillian Skidmore,[2] Nina Li,[1] Heather Myler,[2] Qing Dallas-Yang,[1] Anna-Maria Putnam,[2] Jun Yao,[1] Stuart Bussell,[2] Margaret Wu,[1] Thea C. Norman,[2] Carlos G. Rodriguez,[3] Bruce Kimmel,[2] Joseph M. Metzger,[3] Anthony Manibusan,[2] Darin Lee,[2] Dennis M. Zaller,[4] Bei B. Zhang,[1] Richard D. DiMarchi,[5] Joel P. Berger,[1] and Douglas W. Axelrod[2]

Fibroblast growth factor 21 (FGF21) mitigates many of the pathogenic features of type 2 diabetes, despite a short circulating half-life. PEGylation is a proven approach to prolonging the duration of action while enhancing biophysical solubility and stability. However, in the absence of a specific protein PEGylation site, chemical conjugation is inherently heterogeneous and commonly leads to dramatic loss in bioactivity. This work illustrates a novel means of specific PEGylation, producing FGF21 analogs with high specific activity and salutary biological activities. Using homology modeling and structure-based design, specific sites were chosen in human FGF21 for site-specific PEGylation to ensure that receptor binding regions were preserved. The in vitro activity of the PEGylated FGF21 analogs corresponded with the site of PEG placement within the binding model. Site-specific PEGylated analogs demonstrated dramatically increased circulating half-life and enhanced efficacy in *db/db* mice. Twice-weekly dosing of an optimal FGF21 analog reduced blood glucose, plasma lipids, liver triglycerides, and plasma glucagon and enhanced pancreatic insulin content, islet number, and glucose-dependent insulin secretion. Restoration of insulin sensitivity was demonstrated by the enhanced ability of insulin to induce Akt/protein kinase B phosphorylation in liver, muscle, and adipose tissues. PEGylation of human FGF21 at a specific and preferred site confers superior metabolic pharmacology. ***Diabetes*** **61:505–512, 2012**

The pathobiology of type 2 diabetes (T2D) is heterogeneous and includes alterations in insulin synthesis and target tissue sensitivity. It is commonly accompanied by increased body weight (BW) with associated lipid abnormalities. Current pharmacological treatments have proven insufficient in meeting the full magnitude and diversity of the disease. The utility of newer medications, such as the glucagon-like peptide 1 analogs and dipeptidyl peptidase-4 (DPP-4) inhibitors, demonstrates notable efficacy with enhanced safety, but still falls short of meeting the multiple demands presented by T2D. Most patients eventually progress to a point of being insulin dependent.

Into this setting, a new pleuripotent hormone, fibroblast growth factor 21 (FGF21), came to attention (1) as a potentially important modulator of intermediary metabolism in a variety of pathological settings. As a result, many studies have examined the potential utility of this hormone for the treatment of T2D (2–5). These studies have demonstrated important activity in insulin expression and secretion, tissue sensitivity to insulin, and the resulting carbohydrate and lipid fluxes. As a result, FGF21 holds promise as a multifaceted therapeutic that can address multiple aspects of T2D pathogenesis. As these preclinical studies have progressed, it has also become clear that the native protein has pharmaceutical limitations, a short half-life being one of the more prominent among them. Thus, despite the promise of this therapeutic, this limitation diminishes the attraction for clinical testing and has forestalled development.

In this setting, we examined the utility of applying a biosynthetic approach to site selectively install a unique amino acid that could serve as the site of attachment for a single polyethylene glycol (PEG)–based polymer. This site-directed placement of unique chemical functionality is termed ReCode (6) (reconstituting chemically orthogonal–directed engineering) (Fig. 1). It uses a tRNA that has been modified to recognize the UAG (amber) codon and an evolved aminoacyl tRNA synthetase (*O*-RS), which can charge this tRNA (*O*-tRNA) with a novel amino acid that has chemical attributes orthogonal to those found in the naturally occurring 20 amino acids. In this way, placement of the UAG codon within the DNA encoding a protein of interest can direct site-specific insertion of that novel amino acid into the protein during translation. After purification of the protein, the novel amino acid can be conjugated with complete specificity to an array of conjugates (Fig. 2). In the instance of FGF21, the novel amino acid *p*-acetylphenylalanine (*p*AcF) was used. The ketone side chain functionality of this novel amino acid is uniquely reactive in the protein and when reacted with amino-oxy–functionalized PEG polymer, it results in a stable oxime adduct of the PEGylated protein.

Herein, we describe the identification of site-specific PEGylated FGF21 analogs that demonstrated enhanced efficacy when administrated less frequently than the native hormone. Two of these PEGylated FGF21 variants, when studied in *db/db* mice at a dose and frequency that was BW

From the [1]Department of Metabolic Disease-Diabetes, Merck Research Laboratories, Rahway, New Jersey; the [2]Departments of Preclinical Sciences and Process Development, Ambrx Inc., La Jolla, California; the [3]Department of In Vivo Pharmacology, Merck Research Laboratories, Rahway, New Jersey; the [4]Department of External Discovery and Preclinical Sciences, Merck Research Laboratories, Rahway, New Jersey; and the [5]Department of Chemistry, Indiana University, Bloomington, Indiana.

Corresponding author: Jason Pinkstaff, jason.pinkstaff@ambrx.com.

Received 11 July 2011 and accepted 7 November 2011.

DOI: 10.2337/db11-0838

This article contains Supplementary Data online at http://diabetes.diabetesjournals.org/lookup/suppl/doi:10.2337/db11-0838/-/DC1.

H.M. is currently affiliated with Bristol-Myers Squibb, Princeton, New Jersey. S.B. is currently affiliated with SBPD Consulting, Carlsbad, California. B.K. is currently affiliated with Howard Hughes Medical Institute, Ashburn, Virginia. D.W.A. is currently affiliated with Ambrx Inc., Rancho Santa Fe, California. B.B.Z. is currently affiliated with Eli Lilly, Indianapolis, Indiana.

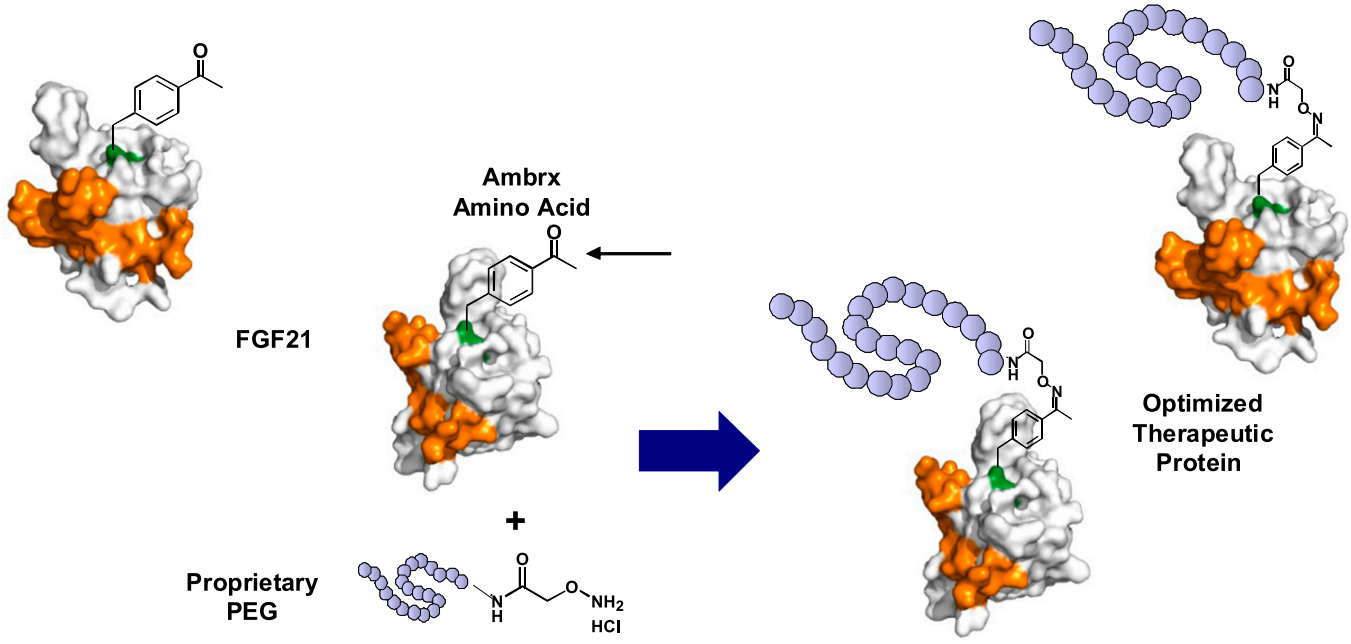

FIG. 1. Protein conjugation with PEG via oxime bond formation. The protein of interest contains a single *p*AcF positioned away from the region(s) important for function, e.g., receptor binding, (shown in orange) to minimize loss of biological activity. The PEG (bead of blue circles) is functionalized with an alkoxy-amine group, which reacts with the ketone functional group on *p*AcF at pH ~4.5 to form an oxime bond as described in RESEARCH DESIGN AND METHODS.

neutral, elicited a robust glucose-lowering activity that was not observed with native hormone. This antidiabetic activity was associated with the ability to increase insulin sensitivity, augment glucose catabolism, maintain pancreatic insulin content, and preserve pancreatic islet mass and function. These results extend our understanding of the physiologic activities of FGF21 while enhancing the potential for FGF21 agonism as a novel mechanism for T2D therapy.

RESEARCH DESIGN AND METHODS

Selection of sites for *p*AcF incorporation. A human FGF21 theoretical model was constructed by homology modeling using the crystal structures of FGF19 (Protein Data Bank code 2P23 and 2PWA) (7,8) and FGF23 (Protein Data Bank code 2P39) (7); all three belong to the FGF19 subfamily. The FGF19 subfamily members use Klotho proteins to facilitate their interactions with FGF receptors (FGFRs), rather than heparin sulfate as other FGF family members (7). Building on previous biochemical and structural work characterizing the FGF family receptor-binding interface (7–10), amino acids with surface-exposed side chains distal from the putative receptor binding regions were selected for substitution with *p*AcF and subsequent PEG attachment.

Cell line construction and production of *p*AcF-containing FGF21Q108amber. Using previously described methods (6), an *Escherichia coli* K-12 W3110 cell line was generated to create a temperature-sensitive cell line with an additional W375R point mutation to confer lethal host phenotype at temperatures ≥37°C, which was subsequently transformed with an FGF21Q108amber plasmid into DH5α-T1 cells (Invitrogen Corp., Carlsbad, CA). FGF21Q108*p*AcF protein production was confirmed through SDS-PAGE and liquid chromatography-mass spectrometry.

GF protein purification and PEGylation. Production and purification of PEGylated His_6-FGF21 variants was accomplished as described earlier (6). The PEGylated His_6-tagged FGF21 protein was >95% pure, with endotoxin levels in each variant <2 EU/mg protein by LAL analysis with EndoSafe-PTS LAL cartridges (Charles River Laboratories, Wilmington, MA).

For production of PEGylated FGF21 variants lacking the His_6 tag, frozen cell paste was resuspended in 9 mL buffer per gram of paste in 50 mmol/L Tris, 100 mmol/L NaCl, 1 mmol/L EDTA, 1% Triton X-100, pH 8.0. The lysate was centrifuged at 10,000 *g* for 15 min at 4°C, and the pellet was washed using the same resuspension and centrifugation steps. Two additional washes were performed in 50 mmol/L Tris, 100 mmol/L NaCl, 1 mmol/L EDTA, pH 8.0. The pellet containing purified inclusion bodies was solubilized in 9 mL buffer per gram of inclusion bodies in 20 mmol/L Tris, 8 mol/L urea, 10 mmol/L β-mercaptoethanol for 1 h at room temperature, and refolded in 20 mmol/L Tris, pH 8.0, at a 9:1 (v/v) ratio of refold buffer:solubilized inclusion bodies at 4°C for 18–24 h. The refolded solution was processed through 0.2-μm filtration, anion-exchange capture (Q-Sepharose high-performance column; 20 mmol/L Tris, pH 8.0, 0–250 mmol/L NaCl gradient) and a hydrophobic interaction column (phenyl Sepharose high-performance column; binding buffer: 20 mmol/L Tris, 0.55 mol/L ammonium sulfate, pH 8.0; elution buffer: 20 mmol/L Tris, 2 mol/L urea, pH 8.0 gradient elution). The PEGylation and post-PEGylation purification methods were as previously described (6). All variant masses for in vitro and in vivo testing are reported as milligrams of protein without inclusion of the mass of any conjugated PEG.

Phosphoextracellular signal–related kinase Meso Scale Discovery assay. HEK293 β-Klotho clone #4 cells were seeded at 100,000 cells/well in a poly-D-Lys–coated 96-well plate and incubated overnight at 37°C and 5% CO_2 to allow cells to adhere. The next day, fivefold serially diluted wild-type (WT) His_6-tagged FGF21 and His_6-tagged PEGylated FGF21 proteins were added to the cells in duplicate for 9 min at 37°C and 5% CO_2. After stimulation, cold lysis buffer containing protease and phosphatase inhibitors was added to the wells and incubated on ice for 25 min to allow complete cell lysis. After centrifugation, the lysate was transferred to a 96-well Phospho/Total-ERK1/2 MultiSpot plate (Meso Scale Discovery, Gaithersburg, MD). Lysates were analyzed on a Meso Scale Discovery SI2400 reader according to protocol, and half-maximal effective concentration (EC_{50}) values were calculated for all proteins. His_6-tagged PEGylated FGF21 proteins were rank ordered by their EC_{50} values. The top five PEGylated FGF21 proteins, lacking the His_6 tag, were also prepared and demonstrated comparable EC_{50}s.

Pharmacokinetic evaluation. Jugular vein–catheterized, male Sprague Dawley rats (Charles River Laboratories) were housed in individual cages in a temperature-controlled environment with a 12-h light-dark cycle with ad libitum access to water and standard rodent chow (Diet 5001; Purina). Rats were administered a single, subcutaneous injection of WT FGF21 or PEG30-FGF21 variants lacking the His_6 tag (0.25 mg/kg). Blood samples were collected at various time points and analyzed by a bridging ELISA (see below) to determine compound concentrations. All experiments were conducted under protocols approved by the Institutional Animal Care and Use Committee of Ambrx, Inc. Pharmacokinetic analyses were performed using WinNonLin software (version 5.0.1; Pharsight) and noncompartmental modeling.

Serum concentration measurements. Standards, quality controls, and samples were spiked into 100% Sprague Dawley rat serum. All standards, quality controls, and study samples were then loaded onto the wells after pretreating 1:50 with assay buffer. The ARX618 in the standards, quality controls, and samples were captured by immobilized anti-PEG monoclonal

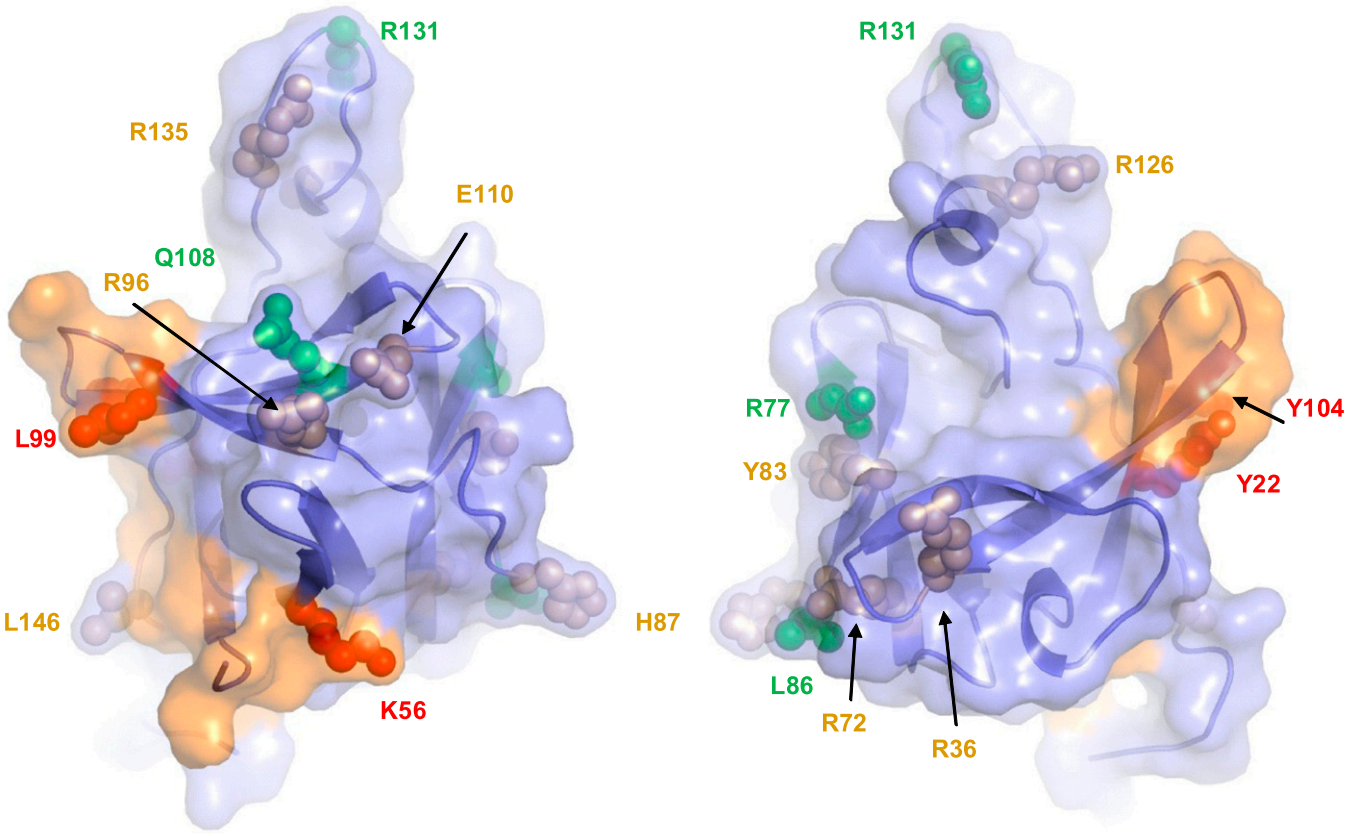

FIG. 2. A theoretical model of FGF21 depicted as a ribbon and semitransparent surface diagram. The structure of the protein is based upon the crystal structures of FGF19 and FGF23. The FGF21 orange surface area contains its theoretical FGFR binding regions based upon the FGF:FGFR cocrystal structure and the known binding relationship of FGFXX with β-Klotho. The specific FGF21 sites into which *p*AcF was inserted are represented as spheres. The colors of the different *p*AcF sites reflect the activity of their PEGylated variants in the cell-based ERK phosphorylation assay (green, sites within the most potent variants; wheat, sites within the modestly potent variants; red, sites within inactive variants). The figure was generated using the PyMOL Molecular Graphics System, version 1.3 (Schrödinger, LLC) as described in RESEARCH DESIGN AND METHODS.

antibody that had been coated onto the plate. After a wash step to remove unbound materials, biotinylated goat anti–FGF21 IgG polyclonal antibody was added to the wells. After another wash step, streptavidin sulfo tag was added for detection of the captured ARX618. After a final wash step, Meso Scale Discovery read buffer was added to all wells, and light was generated in proportion to the amount of ARX618 bound by the capture and detection reagents. The conversion of relative light units for the study samples and the quality controls to concentration was achieved through comparison with a standard curve on the same plate, which was regressed according to a four-parameter logistic regression model with a weighting factor of $1/Y^2$. Results are reported in ng/mL concentration units.

Metabolic studies in *db/db* mice. Male *db/db* mice were purchased at 5 weeks of age from The Jackson Laboratory and housed eight per cage in temperature-, humidity-, and light-controlled rooms with ad libitum access to autoclaved water and food (Diet 5008; Purina). At the beginning of the experiment, *db/db* mice (8 weeks of age) were grouped based on BW and ambient glucose levels. All *db/db* studies were performed with WT FGF21 or PEG30-FGF21 variants lacking the His_6 tag.

For chronic efficacy evaluation, animals were dosed subcutaneously twice weekly (BIW; WT or PEG30-FGF21) or twice daily (BID; WT FGF21) and studied for 12 days. Glucose, BW, and food consumption were monitored as indicated after commencement of treatment. Plasma triglyceride, free fatty acid, insulin, glucagon, and liver triglyceride levels, pancreas staining/quantification, and islet functional studies were performed as previously described (11). Glucagon and insulin were measured using commercial ELISA kits (Linco Research Immunoassay, St. Charles, MO, and ALPCO Diagnostics, Windham, NH, respectively).

For the insulin tolerance test, *db/db* mice (12 weeks of age) were sorted based on blood glucose. Diet was removed at 9:00 A.M. and mice were injected subcutaneously with vehicle or PEG30-FGF21. Humulin R (3 units/kg; Eli Lilly) was administered 6 h afterward. Blood glucose from tail vein was measured by glucometer (Ultra LifeScan; OneTouch, Milpitas, CA) at the indicated time points pre- and postchallenge.

To compare insulin signaling using phospho-Akt as a marker, 12-week-old male *db/db* mice were grouped based on blood glucose. Diet was removed at 9:00 P.M. and mice were injected subcutaneously with vehicle or PEG30-FGF21 at 0.25 mg/kg. Saline or Humulin R (2 units/kg) was injected by tail vein the next morning at 9:00 A.M.. Liver, gastrocnemius muscle, and white and brown adipose tissue were collected 5 min postinjection and snap-frozen in liquid nitrogen for phospho-Akt analysis with the whole-cell lysate phospho-Akt (Ser473) assay kit according to the manufacturer's protocol (Meso Scale Discovery).

Fatty acid synthesis in *db/db* mice. Nine-week-old *db/db* mice received a subcutaneous injection of either vehicle or PEG30-FGF21 at 0.75 mg/kg. One and three hours postdose, mice received an intraperitoneal injection of ^3H-H_2O at 2.5 mCi/kg. Mice were killed 1 h post–^3H-H_2O injection, and hepatic de novo lipogenesis (DNL) was determined as described previously (12).

Nutrient utilization studies. Six-week-old, male *db/db* mice were acclimated to a pathogen-free animal facility for 1 week, where they were maintained at 22°C on a 14-h:10-h light-dark cycle. They were placed in individual boxes within the temperature-controlled chambers of an OxyMax metabolic system (Columbus Instruments, Columbus, OH). The mice were randomized according to their glucose levels and divided into two groups ($n = 8$); one cohort received 0.25 mg/kg PEG30-R131 subcutaneously once daily for 12 days while the other was injected with vehicle. The OxyMax metabolic chamber system ran 24 hours a day, 7 days a week to collect oxygen consumption (V_{O_2}) and CO_2 production (V_{CO_2}) data nonstop except when the mice were dosed right after their dark cycle ended. The respiratory exchange ratio (RER) was calculated as V_{CO_2}/V_{O_2}.

Statistics. All data are expressed as means ± SEM. Statistical analysis was conducted using ANOVA or unpaired Student t test where appropriate. Statistical significance was defined as $P < 0.05$.

RESULTS

Synthesis of PEGylated FGF21 variants. A human FGF21 theoretical model was constructed by homology modeling, using the crystal structures of FGF19 and FGF23

(7,10). Building on previous biochemical and structural work characterizing the FGF family receptor-binding interface (9), amino acids with surface-exposed side chains distal from the putative receptor binding regions were selected for substitution with *p*AcF and subsequent PEG attachment (see RESEARCH DESIGN AND METHODS).

On the basis of the aforementioned modeling, a series of human FGF21 variants was constructed by inserting the novel amino acid *p*AcF at single specific sites within the protein using the ReCode methodology. These variants were then biosynthesized, PEGylated with a 30-kDa PEG, and purified as described in RESEARCH DESIGN AND METHODS. The variants that were generated are listed in Table 1.

Cell-based functional characterization of PEGylated FGF21 variants. His_6-tagged versions of the PEGylated FGF21 variants, designated by the location of the novel amino acid insertion, were tested for in vitro activity by examining their ability to augment extracellular signal–related kinase phosphorylation (pERK) within a HEK293 cell line engineered to stably express β-Klotho. As previously described (7), FGF21 intracellular signaling activity required the endogenous expression of FGFRs and the forced expression of β-Klotho. Table 1 shows the potencies with which His_6-tagged WT FGF21 and the corresponding variants induced pERK levels. There was a good correlation among the variants between pERK activity and location within the homology model. Variants Y22, K56, L99, and Y104, which are all within the modeled FGFR binding sites, proved to be entirely inactive. In contrast, those variants most distal to the binding sites, R77, L86, Q108, and R131, proved to be most potent, whereas other variants were found to be of intermediate activity. The potency of the most active PEGylated proteins was diminished approximately fivefold compared with WT FGF21. Glucose uptake assays performed in 3T3-L1 adipocytes demonstrated the superior potency of a largely overlapping set of variants, R77, L86, E91, Q108, and R131, whereas K56, L99, and Y104 were once again found to be inactive (not shown). Therefore, we found good concordance of PEGylated variant potency using different means of assessing their functional activity in vitro.

TABLE 1
Summary of the HEK293 β-Klotho cell ERK phosphorylation assay

FGF21 variant	EC_{50} (ng/mL)
WT	36 ± 7
R131	173 ± 34
E91	183 ± 66
Q108	201 ± 62
R77	210 ± 70
L86	358 ± 139
R126	398 ± 3
R72	496 ± 251
E110	566 ± 294
Y83	709 ± 0.4
H87	696 ± 492
P146	672
R135	794
R96	1,493
R36	2,055
Y104	>10,000
L99	>10,000
K56	>10,000
Y22	>10,000

Eighteen His_6-tagged PEGylated FGF21 proteins were rank ordered based on their potency. The five most potent PEGylated FGF21 proteins were evaluated without the His_6 tag: no significant change in EC_{50} was observed (not shown). All variants were conjugated with 30-kDa PEG except for WT. WT FGF21 was prepared with and without the His_6 tag to serve as the appropriate comparator for the PEGylated FGF21 proteins. Data from assays performed in replicate are shown as mean ± SD. Variants with no SD values shown were only tested once in the assay.

Pharmacokinetics of PEGylated FGF21 variants. The most potent PEGylated variants, R77, L86, E91, Q108, and R131, were selected for single-dose subcutaneous testing in male rats and prepared without the His_6 tag. As shown in Supplementary Fig. 1, all of these PEGylated proteins had substantially prolonged pharmacokinetic profiles versus the WT protein. Beyond this general PEG effect on circulating FGF21 levels, important differences in pharmacokinetics were seen among the variants conjugated to the same size PEG. For example, compared with the WT FGF21–terminal half-life of 1.19 h, 30-kDa PEG differentially prolonged the half-lives of PEGylated variants across a range extending from 14.72 (R72) to 33.9 h (L86), a greater than twofold difference based solely on the site of attachment. The areas under the curve (AUCs) showed a similar range, with the WT protein displaying an AUC of 259.8 ng · h/mL, whereas those of the PEGylated variants ranged from 3,216 ng · h/mL (L86) to 13,238 ng · h/mL (R126). These differences in circulation time were not predicted from the protein homology modeling, nor did they correlate with measured in vitro activities of the variants. Thus, the specific site of PEGylation can alter pharmacokinetics beyond the choice of PEG size itself. The combination of well-preserved in vitro activity and enhanced plasma levels warranted the further study of these five FGF21 variants in a setting where in vivo efficacy could be determined.

PEG30-FGF21 displays antihyperglycemic efficacy in *db/db* mice without reducing BW. Several previous studies characterizing the actions of WT FGF21 (1,4) have demonstrated its glucose-lowering activity in rodent models that displayed concurrent BW reduction, making it difficult to determine the direct antihyperglycemic activity of the protein. Additionally, these earlier studies had to use aggressive dosing regimens in order to maintain pharmacologically active levels of WT FGF21. To avoid alterations in BW and concerns with the short half-life of WT FGF21, we conducted studies with the PEG30-FGF21 variants Q108 and R131 in *db/db* mice, an obese, hyperphagic model of T2D that lacks a functional leptin receptor. During a 12-day experiment, once-daily subcutaneous dosing of either PEG30-FGF21 analogs lowered ambient glucose robustly at doses as small as 0.1 mg/kg (data not shown). To examine efficacy with an extended dosing interval, mice were dosed subcutaneously BIW with Q108 and R131 and monitored for decreases in glucose over 12 days. When administered at 0.75 and 2.5 mg/kg, both variants dose dependently lowered circulating glucose levels and essentially normalized hyperglycemia at the higher dose (Fig. 3*A*). Unlike results reported in other animal models (1,2,4,5), *db/db* mouse BW was maintained during the course of the study (Fig. 3*B*), supporting the proposition that the decrease in ambient glucose seen in this T2D model was a direct effect and not secondary to BW reduction. Reduction of fasting glucose (Fig. 3*C*) and improved glucose tolerance (data not shown) were also detected during the study, notably without hypoglycemia even at the highest doses. BID dosing of WT FGF21 at 1.25 mg/kg resulted in glucose-lowering efficacy similar to PEG30-Q108 and PEG30-R131 (Fig. 3*D*), whereas BIW dosing of WT FGF21 at 2.5 mg/kg had no effect on ambient glucose; neither dosing paradigm caused BW change (data

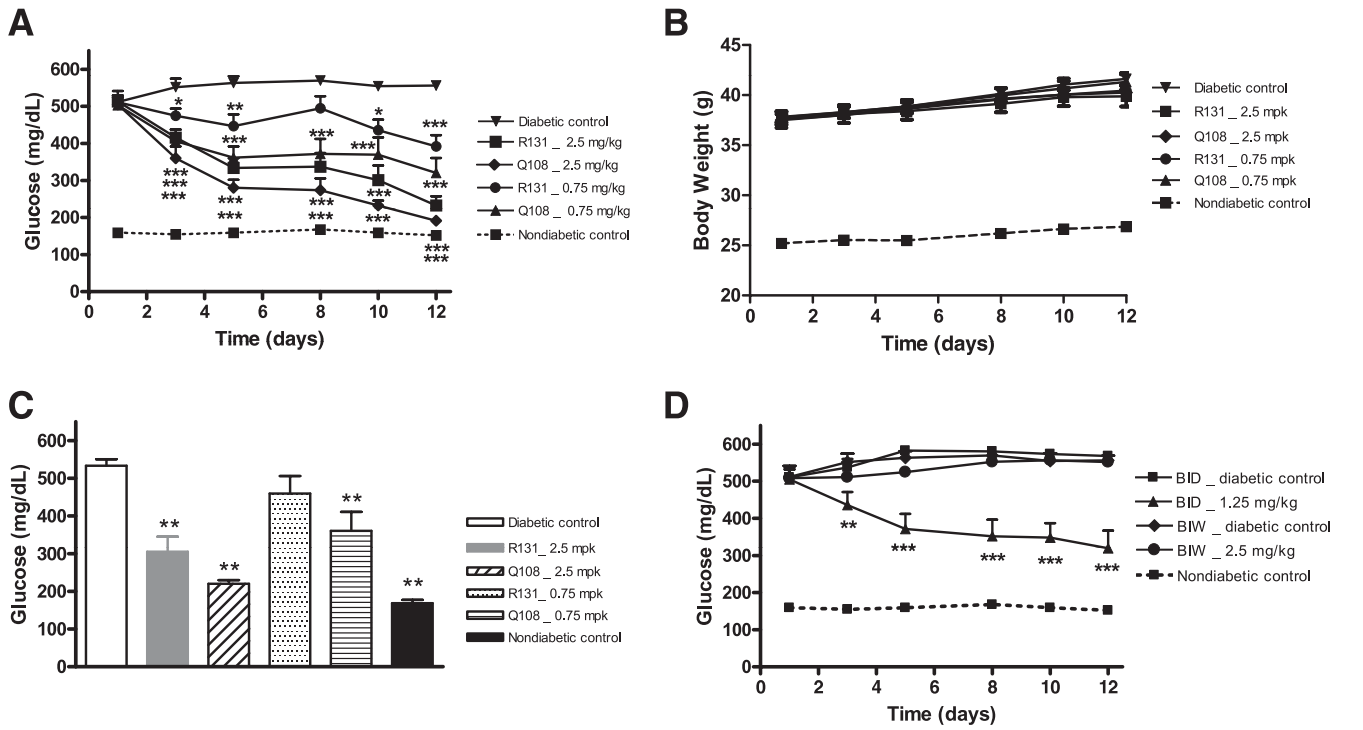

FIG. 3. PEG30-FGF21 variants decrease ambient and fasting hyperglycemia without impacting BW in *db/db* mice. *Db/db* mice were dosed with PEGylated FGF21 variants Q108 and R131 (BIW; 9:00 A.M. on days 1 and 8 and 5:00 P.M. on days 4 and 11) or WT FGF21 (BID or BIW) for 12 days. Fed glucose (*A* and *D*), body weight (*B*), and 6-h fasting glucose (*C*) are shown. *$P < 0.05$, **$P < 0.01$, ***$P < 0.001$ vs. respective control group; $n = 7$.

not shown). Taken together, these results indicate that potent PEG30-FGF21 variants displayed robust antihyperglycemic activity in diabetic mice without affecting their BW. Furthermore, these PEGylated proteins provided comparable efficacy to WT FGF21 when dosed far less frequently and at lower cumulative doses, a likely result of their significant intrinsic activity and greatly increased in vivo half-life.

PEG30-FGF21 improves lipid profile and pancreatic function. In addition to mitigating elevated glucose levels, PEGylated Q108 and R131 both reduced plasma and liver triglyceride levels in *db/db* mice at the termination of the 12-day study (Supplementary Fig. 2*A* and *B*). Additionally, a single injection of PEGylated R131 significantly reduced hepatic DNL as soon as 1 h postdose (Supplementary Fig. 2*C*), thereby providing a potential mechanism for the observed reductions in dyslipidemia and hepatic steatosis.

At the termination of the 12-day study, glucagon levels were significantly reduced in *db/db* mice treated with PEGylated Q108 and R131 (Fig. 4*A*). Pancreatic insulin content (Fig. 4*B*) generally trended higher, with the effect of Q108 reaching statistical significance at 2.5 mg/kg. In comparison with vehicle treatment, PEG30-Q108 increased total islet number from 51.2 ± 6.8 to 98.2 ± 4.2 10E6/mm^2; this augmentation was distributed across the range of observed islet sizes (Fig. 4*C*). In a separate study, *db/db* mice were dosed BIW with PEG30-Q108 at 2.5 mg/kg for 6 days, and islets were subsequently isolated to measure insulin content and secretion; the same number of size-matched islets were isolated and examined from each animal. Significant increases in static islet insulin content (data not shown) and ex vivo glucose-dependent insulin secretion (Fig. 4*D*) were found in islets from PEGylated Q108– versus vehicle-treated mice.

Acute PEG30-FGF21 administration improves insulin sensitivity in *db/db* mice. To determine whether PEG30-FGF21 affects insulin sensitivity in diabetic *db/db* mice before glucose lowering is observed, the animals were given a single injection of PEG30-R131 at 0.25, 0.75, or 2.5 mg/kg. This treatment resulted in reduced fasting plasma insulin and improved insulin tolerance in a dose-responsive manner 12 h postdose (Fig. 5*A–C*). We also profiled phospho-Akt levels in four major metabolic tissues 15 min after an intravenous injection of vehicle or insulin. The results (Fig. 5*D–G*) indicated that a single dose of PEGylated R131, provided 12 h in advance of insulin administration, significantly improved insulin signal transduction in liver, skeletal muscle, and white and brown adipose tissue. Together, these data demonstrated that a single dose of a potent PEG30-FGF21 variant led to a rapid improvement of insulin sensitivity in *db/db* mice without causing hypoglycemia, even at higher doses.

PEG30-FGF21 alters metabolic fuel utilization. After observing the ability of PEG30-FGF21 to dramatically reduce hyperglycemia in *db/db* mice without increasing BW, we hypothesized that the glucose was being taken up by various metabolic tissues and oxidatively catabolized. In order to test this proposition, we placed *db/db* mice in an OxyMax metabolic chamber system and injected them daily for 12 days with 0.25 mg/kg PEG30-R131 while constantly monitoring their V_{O_2} and V_{CO_2}. These measurements were used to calculate the RER of the mice. We found that although both cohorts began the study with an RER of ~0.86, the RER of those treated with the PEG30-FGF21 variant rose to ~0.91 over the course of 4 days and maintained this elevated level throughout the treatment regimen (Fig. 6). In contrast, the control group's RER trended down to ~0.83 during the course of the study. These results demonstrated that treatment of *db/db* mice with PEGylated R131 rapidly and durably increased oxidation of glucose, thereby allowing it to be removed from circulation without accumulating in insulin-responsive tissues as glycogen or lipids that would increase BW.

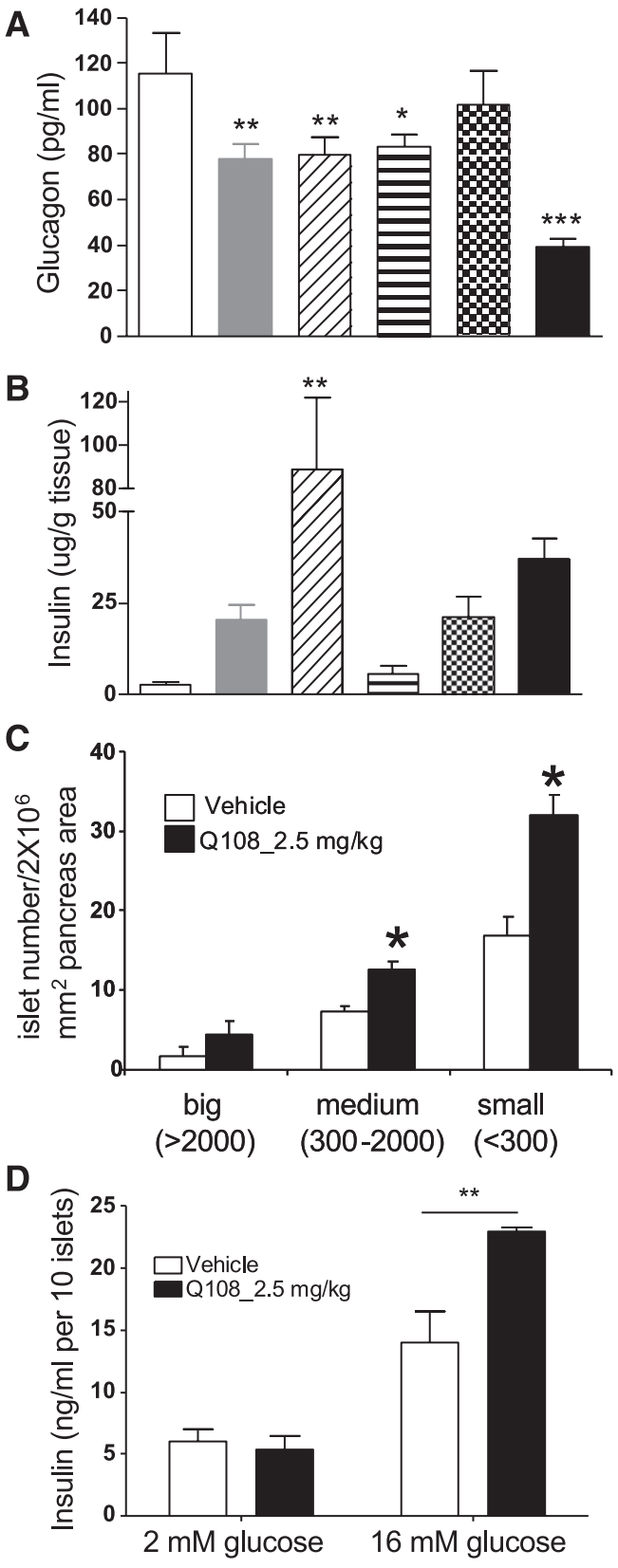

FIG. 4. Effect of chronic PEG30-FGF21 variant treatment on pancreatic hormones and function in *db/db* mice. Plasma glucagon (*A*) levels were measured using the terminal bleed from the 12-day *db/db* study with PEGylated variants Q108 and R131. Pancreatic insulin (*B*) and islet size (*C*) were also analyzed from the same study. Insulin secretion from freshly isolated islets (*D*) was assessed after 6 days of PEGylated Q108 treatment. *$P < 0.05$, **$P < 0.01$, ***$P < 0.001$ vs. respective vehicle controls; $n = 5–7$.

DISCUSSION

Recent studies in preclinical species have shown that FGF21, an atypical endocrine hormone–like member of the FGF superfamily, can address multiple pathophysiologic elements of T2D. These include mitigation of hyperglycemia and insulin resistance, the preservation of insulin production and pancreatic β-cell function, amelioration of dyslipidemia and altered lipid storage, and improvement of intermediary metabolism substrate fluxes (1–5). To our knowledge, no adverse effects of FGF21, including hypoglycemia at high doses, have yet been described in the literature. Thus, FGF21 has emerged as a promising candidate for the treatment of T2D.

Unfortunately, the short duration of circulation and action of native FGF21 undermines its therapeutic utility. Thus, the search for a means of prolonging the pharmacokinetics of FGF21 while maintaining its intrinsic activity led to the utilization of a novel, selective PEGylation strategy. The importance of such selectivity has been amply demonstrated, because conventional PEGylation of therapeutic proteins typically leads to the generation of heterogeneous mixtures, or less than optimal site selection (6). As a result, the specific activity is often reduced relative to the native protein, thereby necessitating higher clinical doses that lead to increased concerns about increased immunogenicity, renal vacuolation, and treatment cost.

Homology modeling allowed directed selection of *p*AcF site incorporation predicted to be distant from the receptor binding regions of human FGF21. Functional characterization of the PEGylated variants using cell-based assays measuring induction of ERK phosphorylation and glucose uptake validated the structural model we had produced, demonstrating that mono-PEGylation of FGF21 with a linear PEG30 polymer at putative receptor binding sites caused large losses in protein potency, whereas PEGylation at sites distal to those involved in FGFR interactions maintained high potency. These findings indicated that site matters in prolonging time of action while maintaining specific activity. Recode methodology enables selection based on biological properties as opposed to conventional approaches rooted in the native placement of lysine. In addition, we showed that the same PEG30 polymer differentially improved the pharmacokinetic character of FGF21, when conjugated to different sites, perhaps due to differential absorption and proteolytic lability. These data collectively illustrated the pharmacological power in being unconstrained in site selection through biosynthesis with unique chemical functionality.

With no detectable weight change upon exposure to WT FGF21 or its PEGylated variants, *db/db* mice served as a good model to assess the direct metabolic actions of this therapy in a stringent rodent model of T2D. We found that BIW administration of the five most potent PEGylated FGF21 variants led to impressive glucose lowering with no sign of hypoglycemia during the 12-day study period. The rank ordering of their glucose-lowering potencies was similar to that observed in the pharmacokinetic study, with the best overall performance demonstrated by variants Q108 and R131. Such data provide strong evidence that FGF21 has direct antihyperglycemic activity and that site-specific mono-PEGylation of FGF21, as described in this work, provided molecular entities with superior pharmacological properties.

Accompanying the antihyperglycemic efficacy, treatment with PEGylated FGF21 analogs preserved pancreatic islet morphology, size, and number and improved

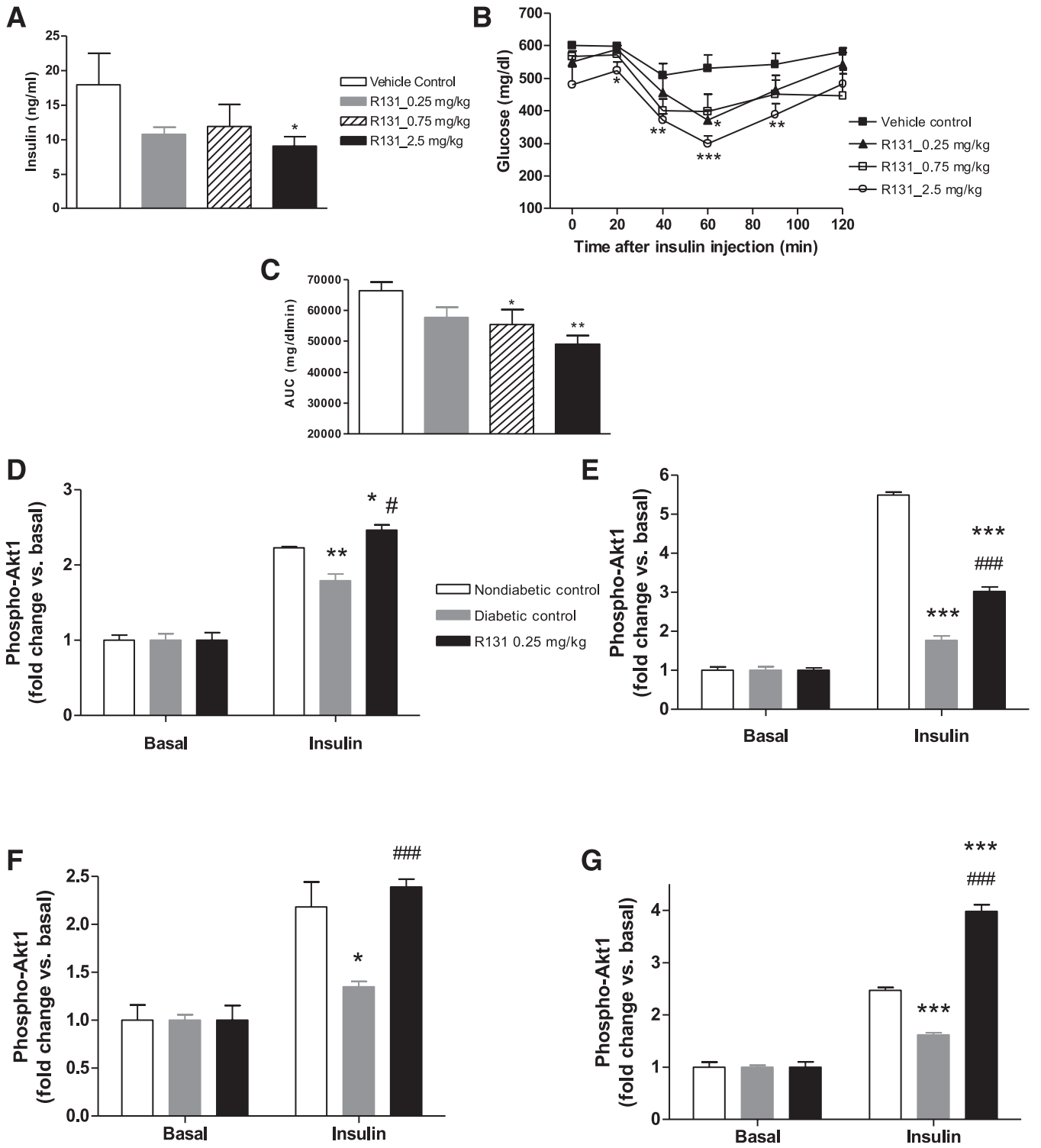

FIG. 5. PEG30-FGF21 improves insulin sensitivity and insulin signaling in *db/db* mice. Mice were subcutaneously dosed once with the PEGylated R131 variant and fasted for 12 h before initiation of an insulin tolerance test (3 units/kg). Fasting plasma insulin (*A*), insulin-induced glucose lowering (*B*), and glucose AUC (*C*) are shown. **P* < 0.05, ***P* < 0.01, ****P* < 0.001 vs. their respective vehicle controls. To examine insulin signaling, mice were subcutaneously dosed with vehicle or PEGylated R131 and fasted for 12 h before an intravenous insulin injection (2 units/kg). Tissues were collected 5 min post-insulin administration and snap frozen. Cleared tissue lysate phospho-Akt1 analysis was conducted using the Phospho-Akt (Ser473) Assay kit from Meso Scale Technology as described in RESEARCH DESIGN AND METHODS. Fold changes of insulin-treated vs. matching vehicle-treated samples were calculated for liver (*D*), skeletal muscle (*E*), white adipose tissue (*F*), and brown adipose tissue (*G*) and are shown as mean ± SEM. **P* < 0.05, ***P* < 0.01, ****P* < 0.001 vs. nondiabetic control; #*P* < 0.05, ###*P* < 0.001 vs. diabetic control; *n* = 7–8.

glucose-dependent insulin secretion. These results are important because loss of islet function and mass are hallmarks of T2D (13), and the ability to mitigate endocrine pancreas deterioration promises durable antidiabetic therapy.

PEGylated FGF21 variants enhanced insulin sensitivity, as was detectable by diminished fasting insulin and improved insulin tolerance as early as 12 h after a single administration and long before significant glucose-lowering efficacy

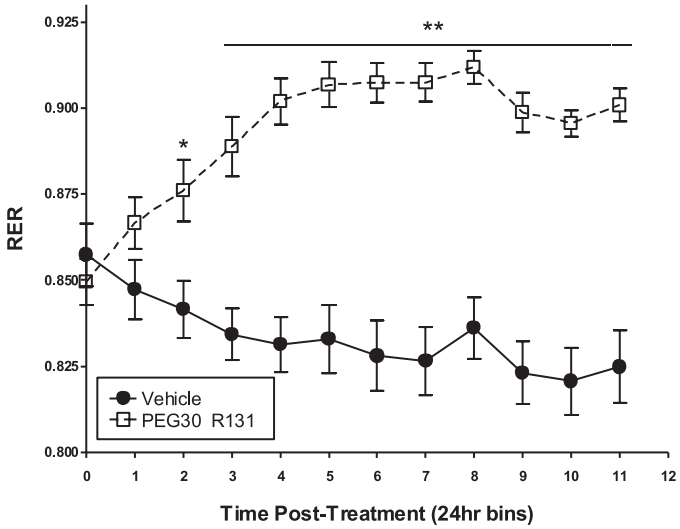

FIG. 6. PEG30-FGF21 treatment elevates the RER of *db/db* mice. The RER was calculated from the ratio of V_{O_2} and V_{CO_2} which were measured continuously in an OxyMax metabolic chamber system during a 12-day study in which mice were subcutaneously dosed with vehicle or 0.25 mg/kg PEGylated R131 daily. *$P < 0.05$ and **$P < 0.01$ vs. vehicle control; $n = 7–8$.

was observed. Additionally, increased insulin sensitivity was manifested by potentiation of insulin-induced Akt phosphorylation in major metabolic tissues, including liver, skeletal muscle, and adipose, which suggests that these tissues mediate the observed FGF21-induced improvements in whole-body insulin sensitivity and glucose disposal.

Acute administration of PEG30-FGF21 resulted in a rapid diminution in DNL. Though modest in scale, this change probably contributed to the reduction in hepatic steatosis seen after chronic treatment with PEGylated FGF21, which in turn would fortify its aforementioned insulin-sensitizing activity. The inhibition of hepatic DNL by PEG30-FGF21 might also mediate the observed improvement in dyslipidemia.

Our work demonstrated that FGF21 can modify nutrient utilization based on the availability of fuel substrate. In particular, when provided to hyperglycemic *db/db* mice, PEG30-FGF21 durably increased whole-body carbohydrate oxidative catabolism as indicated by an elevation in RER. Therefore, we proffer that PEGylated FGF21 enhances metabolic flexibility, i.e., the switch to insulin-stimulated glucose oxidation during periods of elevated circulating glucose, which has previously been shown to be impaired in T2D (14). Alleviating such a metabolic derangement could aid in the mitigation of insulin resistance.

In summary, our findings demonstrate that site-specific PEGylation of FGF21 results in the generation of potent, long-acting molecules with highly desirable antidiabetic therapeutic profiles. Such uniquely modified proteins hold significant promise in addressing the complex syndrome of T2D.

ACKNOWLEDGMENTS

This study was funded by Ambrx, Inc. and Merck Research Laboratories. During the course of the research presented in this article, J.P., L.S., H.M., A.-M.P., S.B., T.C.N., B.K., A.M., D.L., and D.W.A. were employed by Ambrx, Inc. and J.M., Z.L., N.L., Q.D.-Y., J.Y., M.W., C.G.R., J.M.M., D.M.Z., B.B.Z., and J.P.B. were employed by Merck Research Laboratories. R.D.D. is professionally related to Ambrx, Inc. No other potential conflicts of interest relevant to this article were reported.

J.M. and J.P. designed and performed research, analyzed data, and wrote the manuscript. Z.L. performed research and analyzed data. L.S. and N.L. designed and performed research and analyzed data. H.M. designed and performed research, contributed new reagents/analytic tools, and analyzed data. Q.D.-Y. performed research and analyzed data. A.-M.P. designed and performed research and analyzed data. J.Y. performed research and analyzed data. S.B. designed and performed research. M.W. performed research and analyzed data. T.C.N. designed research, analyzed data, and wrote the manuscript. C.G.R. and A.M. performed research and analyzed data. B.K. designed research and analyzed data. J.M.M. designed and performed research and analyzed data. D.L. performed research. D.M.Z. and B.B.Z. designed research. R.D.D. wrote the manuscript. J.P.B. designed research, analyzed data, and wrote the manuscript. D.W.A. analyzed data and wrote the manuscript. J.P. is the guarantor of this work and, as such, had full access to all the data in the study and takes responsibility for the integrity of the data and the accuracy of the data analysis.

The authors gratefully acknowledge Drs. Guoqiang Jiang, Cai Li, and Laurent Audoly (Merck Research Laboratories) for their invaluable assistance during the course of these studies. The authors also thank Nancy Thornberry and Dr. Catherine Straeder (Merck Research Laboratories) for their support in this endeavor.

REFERENCES

1. Kharitonenkov A, Shiyanova TL, Koester A, et al. FGF-21 as a novel metabolic regulator. J Clin Invest 2005;115:1627–1635
2. Kharitonenkov A. FGFs and metabolism. Curr Opin Pharmacol 2009;9:805–810
3. Kliewer SA, Mangelsdorf DJ. Fibroblast growth factor 21: from pharmacology to physiology. Am J Clin Nutr 2010;91:254S–257S
4. Xu J, Lloyd DJ, Hale C, et al. Fibroblast growth factor 21 reverses hepatic steatosis, increases energy expenditure, and improves insulin sensitivity in diet-induced obese mice. Diabetes 2009;58:250–259
5. Xu J, Stanislaus S, Chinookoswong N, et al. Acute glucose-lowering and insulin-sensitizing action of FGF21 in insulin resistant mouse models—Association with liver and adipose tissue effects. Am J Physiol Endocrinol Metab. 25 August 2009 [Epub ahead of print]
6. Cho H, Daniel T, Buechler YJ, et al. Optimized clinical performance of growth hormone with an expanded genetic code. Proc Natl Acad Sci USA 2011;108:9060–9065
7. Goetz R, Beenken A, Ibrahimi OA, et al. Molecular insights into the klotho-dependent, endocrine mode of action of fibroblast growth factor 19 subfamily members. Mol Cell Biol 2007;27:3417–3428
8. Suzuki M, Uehara Y, Motomura-Matsuzaka K, et al. betaKlotho is required for fibroblast growth factor (FGF) 21 signaling through FGF receptor (FGFR) 1c and FGFR3c. Mol Endocrinol 2008;22:1006–1014
9. Harmer NJ, Pellegrini L, Chirgadze D, Fernandez-Recio J, Blundell TL. The crystal structure of fibroblast growth factor (FGF) 19 reveals novel features of the FGF family and offers a structural basis for its unusual receptor affinity. Biochemistry 2004;43:629–640
10. Zhang X, Ibrahimi OA, Olsen SK, Umemori H, Mohammadi M, Ornitz DM. Receptor specificity of the fibroblast growth factor family. The complete mammalian FGF family. J Biol Chem 2006;281:15694–15700
11. Mu J, Woods J, Zhou YP, et al. Chronic inhibition of dipeptidyl peptidase-4 with a sitagliptin analog preserves pancreatic beta-cell mass and function in a rodent model of type 2 diabetes. Diabetes 2006;55:1695–1704
12. Jiang G, Li Z, Liu F, et al. Prevention of obesity in mice by antisense oligonucleotide inhibitors of stearoyl-CoA desaturase-1. J Clin Invest 2005;115:1030–1038
13. Wajchenberg BL. Beta-cell failure in diabetes and preservation by clinical treatment. Endocr Rev 2007;28:187–218
14. Færch K, Vaag A. Metabolic inflexibility is a common feature of impaired fasting glycaemia and impaired glucose tolerance. Acta Diabetol 2011;48:349–353